# Relevance of Collisional Flow Mechanism in Dry Granular Flows

Abraham E. Mineneh and Dave H. Chan
*Department of Civil and Environmental Engineering – University of Alberta, Edmonton, AB, Canada*

ABSTRACT
Experimental studies of dry granular flows on small diameter particles revealed the occurrence of collisional flow mechanism only at low stresses which may imply it has limited relevance in earth's granular flows. However, the mechanism is highly related to particle inertia, and thus both shear rate and particle mass play crucial role in its occurrence. 3D-DEM simulations of plane shear flows conducted here for larger particles showed its importance at higher stresses. Its relevance in debris flows and avalanches are further investigated by assessing a range of values of vertical stress, flow velocity, and particle diameter required for rate-dependent flows.

RÉSUMÉ
Les études expérimentales sur les flux de granulats secs de petits diamètres ont révélé la présence d'un mécanisme de flux par collision pour les faibles efforts verticaux. Ceci peut impliquer une limitation de l'importance de la prise en compte des flux de terre granuleuse. Cependant, le mécanisme est extrêmement dépendant des caractéristiques comme l'inertie, le poids des particules ou encore la vitesse de cisaillement qui jouent un rôle crucial dans la présence de ce phénomène. Une étude 3D DEM sur les surfaces de cisaillement a montré l'importance du phénomène sur les grosses particules soumis à une forte contrainte. En ce qui concerne les flux de débris, et avalanche, une étude plus approfondie a été conduite en supposant une plage de valeur pour l'effort vertical, la vitesse du flux, le diamètre des particules.

## 1 INTRODUCTION

Rapid flow behaviour of dry granular material has been extensively studied in laboratory by conducting ring or annular shear and flume experiments (e.g., Bagnold 1954; Savage and Sayed 1984; Patton et al. 1987; Drake 1988; Klausner et al. 2000; Martino and Davies 2003). Granular flow mechanics has been also studied using DEM simulations of plane shear flows (e.g., Thompson and Grest 1991; GDR MiDi 2004; Da Cruz et al. 2005; Campbell 2002, 2005; Hatano 2007).

Laboratory studies were limited to small size particles and they showed rate-dependent flow behaviour due to collisional mechanism at low stresses. However, no such dependency of shear rate was observed at high stresses (e.g., Hungr and Morgenstern 1984; Kaibori 1986; Vibert et al. 1989; Fukuoka and Sassa 1991). A possible reason for this may be the shear rates at which the experiments conducted were not sufficient to initiate collisional mechanism at high stress for small diameter particles that were tested. This can be explained as follows. Rheological studies of collisional granular flows using experiments (e.g., Bagnold 1954) and adopting kinetic theory of gas (e.g., Lun et al. 1984) suggested that vertical normal stress $(\sigma_n)$ is generally related to void ratio $(e)$, particle density $(\rho_p)$, shear rate $(\dot{\gamma})$, and mean particle diameter $(d)$ by $\sigma_n = f(e)\rho_p(\dot{\gamma}d)^2$ where $f(e)$ is a function of void ratio. This implies that at constant void ratio and vertical normal stress, the required shear rate increases with decrease of particle diameter and the product $\dot{\gamma}d$ is constant. This fact is also supported by experiments conducted for different particle diameters at low stresses (e.g., Hanes and Inman 1985; and Patton et al. 1987). Since $\dot{\gamma}d$ is high at high stress, the required shear rate to cause collisional mechanism in small diameter particles will be very high for higher stresses.

In this paper, DEM simulations of plane shear flows will be conducted for large diameter particles at higher stresses in order to investigate the relevance of collisional mechanism by observing the required shear rates for collisional flows. The findings will be helpful to determine the consideration of collisional mechanism in modeling earth's granular flows.

## 2 DISTINCT ELEMENT MODEL

Three dimensional DEM simulation was carried out using spherical particles with periodic boundaries on the sides, and a servo-controlled wall at the top, see Figure 1. Green and red particles were used to model the top and bottom platforms respectively. The size of the model, length-width-height, was set to 9dx9dx10d containing 912 particles including the boundaries. Size effects were examined by conducting some simulations on sizes of 8dx8dx9d and 8dx8dx8d with total particles of 641 and 552 respectively. The results of the smallest size were a little bit different from the others.

During shear, the bottom red particles moved only horizontally in the negative x-direction at a prescribed shear velocity while the servo-controlled wall at the top moved only up and down relative to the green particles to keep the prescribed vertical normal stress constant. Measurements of stresses, shear rates, and void ratio were taken from a *'measurement sphere'* after the flow reached steady state condition. Each simulation represented a single state of flow in which all measured variables uniformly distributed in the plane shear flow. Since gravity is the main factor for heterogeneity, the minimum applied vertical stress in actual experiments is limited by the value required to neglect the effect of gravity on the variation of vertical stress (Savage and Sayed 1984). In DEM simulations, on the other hand, gravity can be easily eliminated (Da Cruz et al. 2005). The steady uniform plane shear simulations conducted here were also carried out with out gravity.

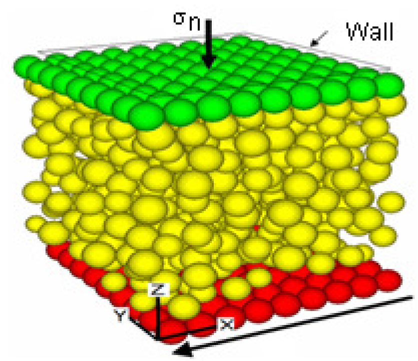


Figure 1. 3D plane shear model.

PFC3D-version 4.0 was used for DEM simulation. The non-linear Hertz-Mindlin contact model was adopted with viscous damping applied in both the normal and shear directions at particle contacts to model inelastic collisions. Forces and relative displacements at a contact in the normal and shear directions are related in case of no viscous damping by Eq.1 (PFC3D-v4.0 User's Guide 2008).

$$F_i^n = K^n U^n n_i \tag{1a}$$

$$\Delta F_i^s = -k^s \Delta U_i^s \tag{1b}$$

$$F_i^s = \min\left(\mu\left|F_i^n\right|, \left|\Sigma\Delta F_i^s\right|\right)\Sigma\Delta F_i^s \Big/ \left|\Sigma\Delta F_i^s\right| \tag{1c}$$

where $F_i^n$ and $F_i^s$ are the total contact normal and shear forces, $U^n$ is the total contact normal displacement, $K^n$ is the contact secant normal stiffness, $n_i$ is a unit vector normal to a contact, $\Delta F_i^s$ is the incremental contact shear force in a time step, $\Delta U_i^s$ is the incremental contact shear displacement, $k^s$ is the contact tangent shear stiffness, and $\mu$ is contact friction coefficient. Contact stiffnesses for Hertz-Mindlin model are given by Eq. 2 (PFC3D-v4.0 User's Guide 2008):

$$K^n = \left(\frac{2\langle G\rangle\sqrt{2\tilde{R}}}{3(1-\langle\nu\rangle)}\right)\sqrt{U^n} \tag{2a}$$

$$k^s = \left(\frac{2\left(\langle G\rangle^2 3(1-\langle\nu\rangle)\tilde{R}\right)^{1/3}}{2-\langle\nu\rangle}\right)\left|F_i^n\right|^{1/3} \tag{2b}$$

$$\tilde{R} = \frac{2R^{[A]}R^{[B]}}{R^{[A]}+R^{[B]}} \tag{2c}$$

$$\langle G\rangle = \frac{1}{2}\left(G^{[A]}+G^{[B]}\right) \tag{2d}$$

$$\langle\nu\rangle = \frac{1}{2}\left(\nu^{[A]}+\nu^{[B]}\right) \tag{2e}$$

where $R^{[A]}$ and $R^{[B]}$ are radii, $G^{[A]}$ and $G^{[B]}$ are shear modulus, and $\nu^{[A]}$ and $\nu^{[B]}$ are Poisson's ratios of the balls in contact.

In case of viscous damping, damping force is added to the contact force given by Eq. 1, and acts to oppose motion. Its normal and shear components are given by (PFC3D-v4.0 User's Guide 2008):

$$D_n = C_n\left|V_n\right| \tag{3a}$$

$$D_s = C_s\left|V_s\right| \tag{3b}$$

where $V_n$ and $V_s$ are relative velocities in normal and shear directions at a contact, and $C_n$ and $C_s$ are damping constants in normal and shear directions which are given by (PFC3D-v4.0 User's Guide 2008):

$$C_n = C_s = \frac{2\sqrt{mk}\ln\varepsilon}{\sqrt{\pi^2 + \ln^2\varepsilon}} \tag{3c}$$

where m, k, and $\varepsilon$ are mass, stiffness, and restitution coefficient of particles respectively. The viscous damping force is calculated after bond breakage and sliding check. If the contact is sliding, then the viscous shear force is reduced to zero. The sum of the contact normal force and the viscous normal force is prevented from becoming attractive between the two involved entities. Hence, the viscous normal force magnitude is limited to $-\left|F_i^n\right|$ (PFC3D-v4.0 User's Guide 2008).

## 3 MODEL CALIBRATION

Since this study is limited to spherical particles, the results of annular shear experiments conducted by Savage and Sayed (1984) on 1 mm mean diameter spherical polystyrene beads were modeled. The sizes of the material were uniformly distributed between 0.81 mm and 1.13 mm (see Figure 2), and the particles had density of 1095 kg/m$^3$. The particles in the simulation were also generated to achieve the same grain size distribution as the polystyrene beads. In order to generate particles assembly of different mean diameter, all particles were scaled by the same percentage to keep the grain size distribution the same. The values of parameters used in the simulation to best fit the experimental results are given in Table 1. The modulus of elasticity (E) and Poisson's ratio $(\nu)$ are close to the actual values of polystyrene material. Restitution coefficient of actual polystyrene beads is estimated to be approximately 0.8 (Farrell et al. 1986).

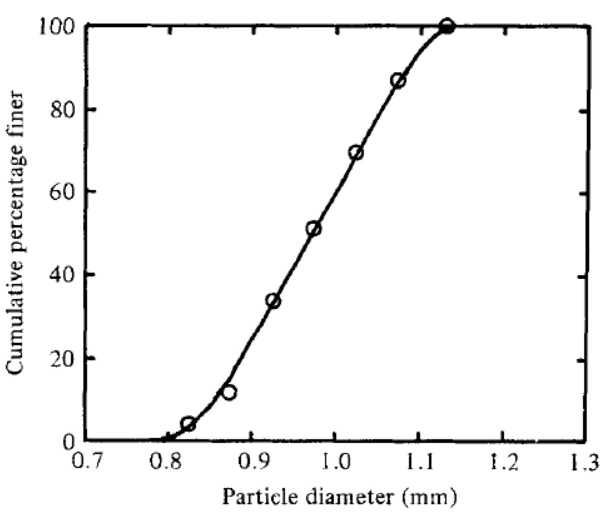


Figure 2. Grain size distribution of polystyrene beads (from Savage and Sayed 1984, Figure 3a)

Table 1. Parameters values for DEM.

| $\rho_p$ (kg/m$^3$) | E (Pa) | $\nu$ | $\mu$ | $\varepsilon$ |
|---|---|---|---|---|
| 1095 | 3.25x10$^9$ | 0.34 | 0.6 | 0.75 |

In order to observe the relation between shear rate and particle diameter at constant void ratio and vertical normal stress, simulations were conducted for particles with mean diameters of 1 mm, 1 cm, and 4 cm at average vertical normal stress of 950 Pa for average void ratios of 0.826 and 1.175, Table 2. The results supported the uniqueness of $\dot{\gamma}d$ at constant void ratio and vertical normal stress. Also, the simulations of 1 mm mean diameter particles are well compared to the experiments. Since we are interested at larger particles, the rest of simulations were conducted for 4 cm mean diameter particles. Then to compare with experimental results (Savage and Sayed 1984, Figures 8a and b), the required shear rates for 1 mm mean diameter particles were taken as 40 times the required shear rates for 4 cm mean diameter particles, see Figure 3.

The major difference in the comparison is that experimental results at average void ratio of 0.908 could not be simulated by the DEM model at the same void ratio. Instead, they were simulated at average void ratio of 0.826. The experimental results at average void ratio of 1.169 were also a little bit over predicted. However, this is the best fit obtained from different trials, and we consider the model is acceptable to use for prediction at higher stresses.

Table 2. Simulations of different mean diameter particles. D & H are experimental results from Savage and Sayed 1984.

| ID | Void Ratio | $\sigma_n$ (Pa) | d (m) | $\dot{\gamma}$ (s$^{-1}$) | $\dot{\gamma}d$ (m/s) |
|---|---|---|---|---|---|
| A | 1.181 | 937 | 0.04 | 12.47 | 0.499 |
| B | 1.188 | 921 | 0.01 | 49.6 | 0.496 |
| C | 1.198 | 905 | 0.001 | 494.8 | 0.495 |
| D | 1.169 | 966 | 0.001 | 570 | 0.57 |
| E | 0.823 | 970 | 0.04 | 6.19 | 0.248 |
| F | 0.824 | 924 | 0.01 | 24.87 | 0.249 |
| G | 0.828 | 900 | 0.001 | 245 | 0.245 |
| H | 0.908 | 967 | 0.001 | 237 | 0.237 |

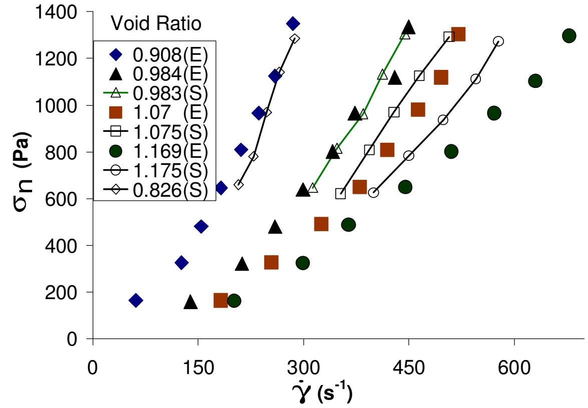


(a)

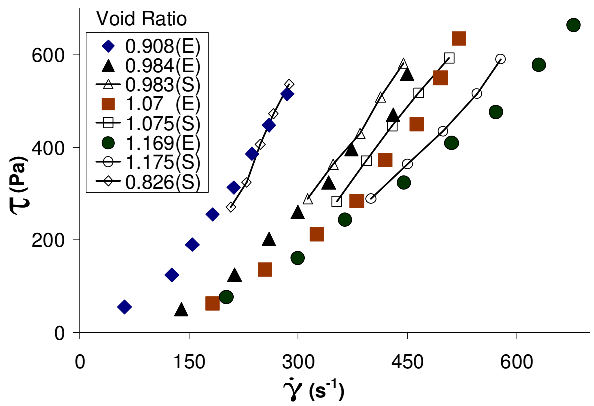


(b)

Figure 3. Comparison of experimental versus simulation results. Simulation results are denoted by (S) while experimental results (taken from Savage and Sayed 1984, Figures 8a and b) are denoted by (E) in the legend. $\tau$ is the shear stress.

## 4 RELEVANCE OF COLLISIONAL MECHANISM

In order to study the relevance of collisional mechanism, simulation using 4 cm mean diameter particles at average void ratio of 1.175 were extended to higher stresses as shown in Figure 4. All flow states lie on a line of slope 2 in Log-Log plot indicating that all belong to pure collisional flow because stresses are related to the square of $\dot{\gamma}d$. The required shear rates for vertical stresses of up to 75 kPa are less than 120 $s^{-1}$, which are within the range of shear rates in rapid debris and rock avalanches.

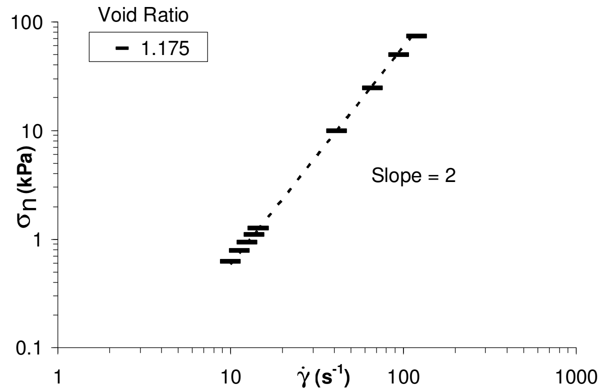


Figure 4. Vertical normal stress versus shear rate for 4 cm mean diameter particles.

In order to assess the required shear rates for small mean diameter particles at these stress levels, the variation of shear rate with particle diameter was first studied at high stress by conducting simulations for 1 mm, 1 cm, and 4 cm mean diameter particles at vertical normal stress of 25 kPa, Table 3. The results confirm again the uniqueness of the quantity $\dot{\gamma}d$. This helps to estimate the shear rates required for 1 mm mean diameter particles at high stresses by multiplying the shear rates in Figure 4 by 40 since 4 cm is 40 times 1 mm. This would give values greater than 1000 $s^{-1}$ which are normally difficult to achieve in actual flows. For example, a shear rate of 2916 $s^{-1}$ is required at 25 kPa, see Table 3. This shear rate is also very difficult to achieve in laboratory experiments. That is why this mechanism was not observed experimentally for small mean diameter particles at higher stresses (e.g., Hungr and Morgenstern 1984; Kaibori 1986; Vibert et al. 1989; Fukuoka and Sassa 1990).

Table 3. Simulation results at vertical stress of 25kPa

| ID | Void Ratio | $\sigma_n$ Pa) | d (m) | $\dot{\gamma}$ ($s^{-1}$) | $\dot{\gamma}d$ (m/s) |
|---|---|---|---|---|---|
| A | 1.174 | 24665 | 0.04 | 66.29 | 2.65 |
| B | 1.177 | 24389 | 0.01 | 263.4 | 2.64 |
| C | 1.168 | 24856 | 0.001 | 2649 | 2.65 |

The above results may indicate that collisional flow mechanism is still relevant in rapid granular flows involving large diameter particles.

For easy interpretation of Figure 4, the results are replotted in Figure 5 by changing the vertical normal stress to flow depth, and shear rate to mean flow velocity as follows. Vertical stress at the base of dry granular flow can be calculated from

$$\sigma_n = \rho_p \upsilon_s g H$$

(4)

where $\upsilon_s$ is the depth average solid fraction, and H is the flow thickness. The depth variations of flowing velocity and density have been studied in inclined planes using laboratory flume experiments (e.g., Johnson 1987; Drake 1988; Ahn 1989; Azanza et al. 1999; Ancey 2001) and simulation experiments (e.g., GDR MiDi 2004) under different conditions. Low variations of solid fraction observed in some cases where it sharply increases for few depths from the surface and then stays nearly constant down to the base. The highest variation of solid fraction also observed in other cases as it increases linearly from zero or minimum value at the surface to a maximum value at the base of flow. Therefore, the depth average solid fraction can vary from $0.5\upsilon_s^b$ to $\upsilon_s^b$ (solid fraction at the base). On the other hand, flow velocity increases approximately linearly from zero or some slip velocity at the base, and its variation becomes more concave near the surface deviating from a linear relationship. But in some cases, for example in smooth flow base, the slip velocity can be very high and the flow velocity is nearly constant for the entire depth. We assume here that

$$\upsilon_s = 0.75\upsilon_s^b \quad (5a)$$

to calculate the corresponding flow thickness from vertical stress at the base using Equation 4. The void ratio at the base is 1.175. We also assume the entire mass undergoes collisional motion, and there exists linear variation of flow velocity and minimum slip velocity so that the depth average velocity $(\overline{U})$ would act at the mid depth of flow, and shear rate (slope of vertical velocity profile) would be constant inside the flowing mass. Therefore, shear rate of flow would be given by

$$\dot{\gamma} = \overline{U}/(H/2) = 2\overline{U}/H \quad (5b)$$

Since Figure 4 was to present simulation results for 4 cm mean diameter particles, vertical normal stress was plotted against shear rate. To generalize for different mean diameter particles, however, the stresses could be plotted against the product $\dot{\gamma}d$. This term is changed to $\overline{U}d$ in Figure 5 by multiplying Equation 5b by d and rewriting as

$$\overline{U}d = \dot{\gamma}d(H/2) \quad (5c)$$

The maximum mean velocities in debris and rock avalanches could reach up to 40 m/s and 100 m/s respectively (Pierson and Costa 1987) while it is estimated for snow avalanche to be 50 m/s (Vilajosana et al. 2007).

If we consider rounded granular material having similar properties to the polystyrene beads, we may able to estimate depths of the material flowing at void ratio of 1.175 for different mean flow velocities, Figure 5. For example, 5 cm mean diameter rock avalanche flowing at 40 m/s may attain flow thickness of 3 m. But 1 mm mean diameter snow avalanche flowing at the same mean velocity may exhibit flow thickness of only 20 cm. If it is required to flow at higher thickness, either the void ratio must decrease or the flowing velocity must increase. However, the collisional mechanism would not exist at very low void ratio, and snow avalanche rarely flows higher than 40 m/s. Therefore, collisional flow mechanism is more important in rapid granular flows involving large particles such as debris and rock avalanches even under significant flow depths. Figure 5 helps to easily visualize the relevance of collisional mechanism by estimating flow depths and velocities instead of stresses and shear rates in Figure 4.

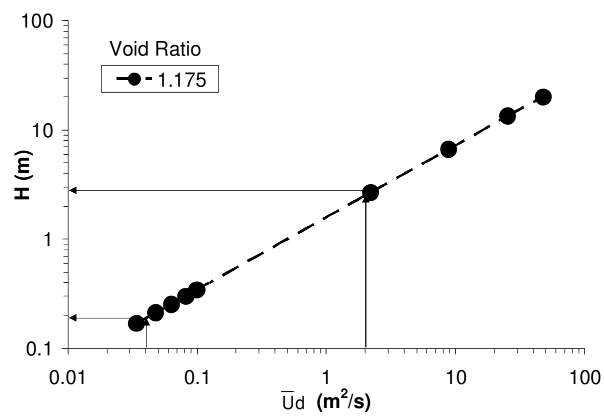


Figure 5. Flow thickness versus $\overline{U}d$.

## 5 CONCLUSIONS

This paper demonstrates that collisional mechanism is one of the flow mechanisms in debris and rock avalanches. The initiation of collisional flow depends on the combination of vertical normal stress, shear rate, particle size and void ratio. It is shown that:

1. The DEM model predicted the general trends of experimental results; the increase of stress with shear rate at constant void ratio, and the increase of stress with decrease of void ratio at constant shear rate. It also fairly predicted the values of stresses and shear rates at average void ratios of 1.169, 1.07, and 0.984. But, these values at average void ratio of 0.908 were predicted for average void ratio of 0.826.
2. DEM simulations at higher stresses indicated that collisional flow mechanism may still be relevant in rapid

granular flows involving large particles as the required shear rate drops with increase of particle size.

3. Collisional flow mechanism is relevant in rapid granular flows such as debris and rock avalanches even under significant flow thicknesses.

## ACKNOWLEDGMENT

The authors would like to acknowledge for the permission granted to reprint the grain size curve (Figure 2) and replotting the data (in Figure 3) from *'Stresses developed by dry cohesionless granular materials sheared in an annular shear cell,'* by S. B. Savage and M. Sayed Journal of Fluid Mechanics, Volume 142, May 1984, pp 391-430 Copyright © 1984 Cambridge University Press. Reprinted with permission

## REFERENCES

Ahn, H. 1989. *Experimental and analytical investigations of granular materials: Shear flow and convective heat transfer*. Ph.D. thesis, California Institute of Technology, Pasadena, California.

Ancey, C. 2001. Dry granular flow down an inclined channel: Experimental investigations on the frictional-collisional regime. *Physical Review E*, 65: 011304 (1-19). DOI: 10.1103/PhysRevE.65.011304.

Azanza, E., Chevoir, F., and Moucheront, P. 1999. Experimental study of collisional granular flows down an inclined plane. *Journal of Fluid Mechanics,* 400: 199-227.

Bagnold, R. A. 1954. Experiments on a gravity-free dispersion of large solid spheres in a Newtonian fluid under shear. *Proceedings of the Royal Society of London, Series A, Mathematical and Physical Sciences*, 225(1160): 49-63. Available from http:// links.jstor.org/sici?sici=0080-4630%2819540806%292 25%3A1160%3C49%3AEOAGDO%3E2.0.CO%3B2-W. [Accessed 7 August 2007].

Campbell, C. S. 2002. Granular shear flows at the elastic limit. *Journal of Fluid Mechanics*, 465: 261-291. DOI: 10.1017/S002211200200109X.

Campbell, C. S. 2005. Stress-controlled elastic granular shear flows. *Journal of Fluid Mechanics,* 539: 273–297. doi:10.1017/S0022112005005616.

Da Cruz, F., Emam, S., Prochnow, M., Roux, J.N., and Chevoir, F. 2005. Rheophysics of dense granular materials: Discrete simulation of plane shear flows. *Physical Review E,* 72(021309): 1-17. DOI: 10.1103/PhysRevE.72.021309.

Drake, T. G. 1988. *Experimental flows of granular material*. Ph.D. thesis, University of California, Los Angeles.

Farrell, M., Lun, C. K. K., and Savage, S. B. 1986. A simple kinetic theory for granular flow of binary mixtures of smooth, inelastic, spherical particles. *Acta Mechanica*, 63: 45-60

Fukuoka, H., and Sassa, K. 1991. High-speed high-stress ring shear tests on granular soils and clayey soils. Rice, Raymond M., technical coordinator. *Proceedings of the IUFRO Technical Session on Geomorphic Hazards in Managed Forests*, Montreal, Canada. Gen. Tech. Rep. PSW-GTR-130, Berkeley, CA: Pacific Southwest Research Station, Forest Service, U.S. Department of Agriculture, 33-41. Available from http://www.treesearch.fs.fed.us/pubs /27325. [Accessed 3 May 2010].

GDR MiDi. 2004. On dense granular flows. *European Physical Journal E*, 14: 341-365. DOI:10.1140/epje/i2003-10153-0.

Hanes, D. M., and Inman, D. L. 1985. Observations of rapidly flowing granular-fluid materials. *Journal of Fluid Mechanics*, 150: 357-380

Hatano, T. 2007. Power-law friction in closely packed granular materials. *Physical Review E*, 75(060301 R): 1-4. DOI: 10.1103/PhysRevE.75.060301.

Hungr, O., and Morgenstern, N. R. 1984. High velocity ring shear tests on sand. *Geotechnique*, 34(3): 415-421.

Itasca Consulting Group, Inc. 2008. *PFC3D Particle Flow Code in 3 Dimensions*. User's Guide, Version 4, Minneapolis, MN, USA.

Johnson, P. C. 1987. *Frictional-collisional equations of motion for particulate flows with application to chutes and shear cells.* Ph.D. thesis, Department of Chemical Engineering, Princeton University

Kaibori, M. 1986. *Study on the movement of the slope failure materials.* Ph.D. thesis, Faculty of Agriculture, Kyoto University.

Klausner, J. F., Chen, D., and Mei, R. 2000. Experimental investigation of cohesive powder rheology. *Powder Technology*, 112: 94-101.

Lun, C. K. K., Savage, S. B., Jeffrey, D. J., and Chepurniy, N. 1984. Kinetic theories for granular flow: inelastic particles in Couette flow and slightly inelastic particles in a general flow field. *Journal of Fluid Mechanics*, 140: 223-256

Martino, R., and Davies, T.R. 2003. Dynamic friction coefficient of a fluid-solid mixture. *International Conference on Fast Slope Movements Prediction and Prevention for Risk Mitigation*, Associazione Geotecnica Italiana, Naples, 1: 357-359.

Patton, J. S., Brennen, C.E., and Sabersky, R.H. 1987. Shear flows of rapidly flowing granular materials. *Journal of Applied Mechanics*, 54: 801–805.

Pierson, T.C., and Costa, J.E. 1987. A rheological classification of subaerial sediment water flows. *Reviews in Engineering Geology*, Geological Society of America, 7**:** 1-12.

Savage, S. B., and Sayed, M. 1984. Stresses developed by dry cohesionless granular materials in an annular shear cell. *Journal of Fluid Mechanics*, 142: 391-430

Thompson, P. A., and Grest, G. S. 1991. Granular Flow: Friction and the dilatancy transition. *Physical Review Letters*, 67: 1751-1754

Vibert, C., Sassa, K., and Fukuoka, H. 1989. Friction characteristics of granular soils subjected to high

speed shearing. *Proceedings of the Japan-China symposium on landslides and debris flows*, The Japan Landslide Society and The Japan Society of Erosion Control Engineering, Niigata and Tokyo, 1: 295-299.
Vilajosana, I., Khazaradze, G., Suriñach, E., Lied, E., and Kristensen, K. 2007. Snow avalanche speed determination using seismic methods. *Cold Regions Science and Technology,* 49: 2-10.